ELSEVIER

Surface Science 511 (2002) 1–12

SURFACE SCIENCE

www.elsevier.com/locate/susc

Applicability of the broken-bond rule to the surface energy of the fcc metals

I. Galanakis [a,*], N. Papanikolaou [b], P.H. Dederichs [a]

[a] *Institut für Festkörperforschung, Forschungszentrum Jülich GmbH, D-52425 Jülich, Germany*
[b] *Fachbereich Physik, Martin-Luther Universität, Halle-Wittenberg, D-06099 Halle, Germany*

Received 23 November 2001; accepted for publication 12 March 2002

Abstract

We apply the Green's function based full-potential (FP) screened Korringa–Kohn–Rostoker method in conjunction with the local density approximation to study the surface energies of the noble and the fcc transition and sp metals. The orientation dependence of the transition metal surface energies can be well described taking into account only the broken bonds between first neighbors and quite similar to the behavior we recently found for the noble metals [I. Galanakis et al., Europhys. Lett., in press]. The (1 1 1), (1 0 0) surfaces of the sp metals show a jelliumlike behavior but for the more open surfaces we find again the noble metals behavior but with larger deviations from the broken-bond rule as compared to the transition metals. Finally we show that the use of the FP is crucial to obtain accurate surface energy anisotropy ratios for the vicinal surfaces.

Keywords: Density functional calculations; Green's function methods; Surface energy; Metallic surfaces; Single crystal surfaces

1. Introduction

The surface energy is a fundamental solid state property since it determines the equilibrium shape of a mesoscopic crystal and plays a decisive role in phenomena like roughening, faceting and crystal growth. Despite of their importance, surface energies are difficult to determine experimentally and just few data exist [1]. Most of these experiments are performed at high temperatures and contain uncertainties of unknown magnitude [1]. The most comprehensive experimental data stem from the extrapolation to zero temperature of surface tension measurements on the liquid [2,3], which cannot provide orientation specific information. Gold crystallites [4] and surfaces [5] have attracted a lot of attention aiming to study the orientation dependence of the surface energy, but these experiments, as it was also the case for experiments on In and Pb crystallites [6], are performed at high temperatures so that the results are difficult to interpret. Entropy terms, describing the lower vibrational frequencies of the atoms at the surface as compared to the bulk, the formation of kinks and finally the creation of holes and pillboxes at the low-index surfaces have to be added to the total free energy. At such high temperatures the surface-melting faceting [7], i.e. the break-down of a vicinal surface in a dry and a melted one, plays a

* Corresponding author. Tel.: +49-2461-616106; fax: +49-2461-612620.
E-mail address: i.galanakis@fz-juelich.de (I. Galanakis).

0039-6028/02/$ - see front matter
PII: S0039-6028(02)01547-9

predominant role. Also the measurement of core level shifts at the surface has been proposed as an indirect measurement of the surface energy anisotropy [8]. Recently, Bonzel and Edmundts [9] have shown that analyzing the equilibrium shape of crystallites at various temperatures by scanning tunneling microscopy can yield absolute values of the surface energies versus temperature, but this technique has not yet been applied.

During the last years there have been several attempts to calculate the surface energy of metals using either ab initio techniques [10–12], tight-binding (TB) parameterizations [13,14] or semi-empirical methods [15,16]. Methfessel and collaborators were the first to study the trends in the surface energy, work function and relaxation for the whole series of bcc and fcc 4d transition metals [10], using a full-potential (FP) version of the linear muffin-tin orbitals (LMTO) method in conjunction with the local-spin density approximation to the exchange-correlation potential [17,18]. In the same spirit Skriver and co-workers have used a Green's function LMTO technique [19] to calculate the surface energy and the work function of most of the elemental metals [11, 12,20]. Recently, Vitos and collaborators [22], using their full-charge density (FCD) Green's function LMTO technique in the atomic sphere approximation (ASA) [23] in conjunction with the generalized gradient approximation (GGA) [24], constructed a large database that contains the low-index surface energies for 60 metals in the periodic table [25]. Their results present a mean deviation of 10% from the FP results by Methfessel and collaborators for the 4d transition metals [26]. Afterwards, they have used this database in conjunction with the pair-potential model [27] to estimate the formation energy for monoatomic steps on low-index surfaces for an ensemble of the bcc and fcc metals [28].

In Ref. [29] we have demonstrated that the surface energies of noble metals scale accurately with the number of broken bonds between first neighbors. Although such a rule has been very often assumed to describe the fcc metals when developing models, no verification by experiments or by ab initio methods exist. This broken-bond rule is very useful for the estimation of the surface energies of vicinal surfaces and of the step energies; the latter ones can be calculated as the energy difference between a vicinal and a flat surface. In this contribution we investigate the question whether the broken-bond rule can also be applied to the surface energies of the other paramagnetic fcc metals: the transition metals Rh, Pd, Ir and Pt, and the sp metals Ca, Sr, Al and Pb. To calculate the surface energies we used the recently developed screened Korringa–Kohn–Rostoker (KKR) method which has been already used to calculate the magnetic properties of 4d monoatomic rows on Ag vicinal surfaces [30]. In Section 2 we describe the details of our calculations and analyze the convergence of our results. We also discuss the importance of relativistic effects. In Section 3, we present the surface energies of the transition and sp metals and discuss the applicability of the broken-bond rule for these systems. All results of Section 3 are obtained by accounting for relativistic effects in the scalar-relativistic (SR) approximation. Finally we discuss the use of the FP instead of the ASA. In the following the symbol Γ is used when we refer to the surface energy in eV/atom and the symbol γ when we refer to the surface energy in $\mathrm{J\,m^{-2}}$.

2. Method of calculation

2.1. Computational details

To perform the calculations, we used the Vosko, Wilk and Nusair parameterization [31] for the local density approximation (LDA) to the exchange-correlation potential [17] to solve the Kohn–Sham equations within the screened KKR method that was recently developed in our group [32]. Its main advantage is that it can treat two-dimensional (2D) and 3D systems in the same footing. Both the ASA [23] and the capability to treat the FP are implemented in this scheme. The ASA calculations take into account the FCD. It was shown by Andersen and collaborators that the charge density obtained in this way for spherically symmetric potentials is close to the density obtained using a FP method [33]. The FP is implemented by using a Voronoi construction of

Wigner–Seitz polyhedra that fill the space as described in Ref. [34]. A repulsive muffin-tin potential (4 Ry high) is used as reference system to screen the free-space long-range structure constants into exponentially decaying ones [35]. For the screening we took for all metals interactions up to the second neighbors into account leading to a "TB" cluster around each atom of 19 neighbors. To calculate the charge density, we integrated along a contour on the complex energy plane, which extends from the bottom of the band up to the Fermi level [36]. Due to the smooth behavior of the Green's functions for complex energies, only few energy points are needed; in our calculations we used 27 energy points. For the Brillouin zone (BZ) integration, special points are used as proposed by Monkhorst and Pack [37]. Only few tens of $\mathbf{k}_{\|}$ are needed to sample the BZ for the complex energies, except for the energies close to the real axis near the Fermi level for which a considerably larger number of $\mathbf{k}_{\|}$-points is needed. Here we used from $\sim$300 points for the vicinal surfaces up to $\sim$800 points for the (1 1 0) surface. In addition we used a cut-off of $\ell_{\max} = 6$ for the multipole expansion of the charge density and the potential and a cut-off of $\ell_{\max} = 3$ for the wave functions. Finally in our calculations the core electrons are allowed to relax during the self-consistency.

To simulate the surface we used a slab with N metal layers and N_{vac} vacuum layers from each side. We have increased the number of metal and vacuum layers such that our surface energies are converged within 0.01 eV. The number of layers needed to converge the surface energies increases with the roughness of the surface and we had to use 12 layers of the fcc metal for the (1 1 1) surface, 14 for the (1 0 0), 18 for the (1 1 0), 21 for the (3 1 1), 30 for the (3 3 1) and the (2 1 0) surfaces. For all these orientations the effective thicknesses of the slabs used in the converged calculations are well comparable and vary from 6.3 up to 7 times the lattice constant. We have also used three vacuum layers from each side of the slab. For all the systems studied we used the experimental lattice parameters: 3.80 Å for Rh, 3.89 Å for Pd, 3.84 Å for Ir, 3.92 Å for Pt, 5.58 Å for Ca, 6.08 Å for Sr, 4.05 Å for Al and finally 4.95 Å for Pb [38]. These numbers differ around 0.1 Å from the numbers used in Ref. [25] where the theoretical GGA equilibrium lattice constants have been used.

2.2. Stability of anisotropy ratios

To test our convergence we present in Table 1 the SR ASA low-index surface energies of Ag and the anisotropy ratios with respect to the different parameters used in the program. The absolute values of the energies change less than 0.01 eV and the anisotropy ratios change by less than 1%. The largest effect comes from the $\ell_{\max}$ cut-off for the wave functions, but globally the first set of parameters is sufficient to give accurate values of both the surface energies and the anisotropy ratios. The second test presented in Table 2 concerns the effect of the lattice parameter on the surface energies and on the anisotropy ratios. Our test has been also performed for the noble metals in SR ASA. Using Cu as a test case, the absolute values

Table 1
SR surface energies in eV/(surface atom) and anisotropy ratios in parenthesis for Ag within ASA using different values for (i) the $\ell_{\max}$ cut-off (LM) for the wave functions, (ii) the size of the TB cluster, (iii) the number of energy points (EN) to perform integrations in the complex energy plane and (iv) the number of $\mathbf{k}_{\|}$-points in the full 2D BZ

LM	TB	EN	KP	Ag(1 1 1)	Ag(1 0 0)	Ag(1 1 0)
3	19	27	55 × 55	0.641	(1.34) 0.860	(1.98) 1.271
3	55	27	55 × 55	0.637	(1.34) 0.854	(1.98) 1.262
3	19	41	55 × 55	0.643	(1.33) 0.855	(1.97) 1.266
3	19	27	75 × 75	0.648	(1.33) 0.860	(1.96) 1.273
3	55	41	75 × 75	0.642	(1.32) 0.849	(1.96) 1.259
4	19	27	55 × 55	0.649	(1.35) 0.879	(2.00) 1.301

The $\ell_{\max}$ cut-off for the charge density is two times the LM value. The first set of parameters is the one used in the following calculations.

Table 2
Effect of lattice parameter changes on the SR ASA surface energies for the three low-index surfaces of Cu in the upper panel and for the (1 1 1) surface of Cu, Ag and Au in the bottom panel

$\frac{a_{exp}-a}{a_{exp}}$	Cu(1 1 1)		Cu(1 0 0)		Cu(1 1 0)	
	Γ (eV)	$\frac{\Gamma_{exp}-\Gamma}{\Gamma_{exp}}$	Γ (eV)	$\frac{\Gamma_{exp}-\Gamma}{\Gamma_{exp}}$	Γ (eV)	$\frac{\Gamma_{exp}-\Gamma}{\Gamma_{exp}}$
0%	0.737		0.982		1.455	
1%	0.730	0.95%	0.971	1.12%	1.441	0.96%
2%	0.719	2.44%	0.956	2.65%	1.420	2.41%
3%	0.706	4.21%	0.939	4.38%	1.394	4.19%
	Cu(1 1 1)		Ag(1 1 1)		Au(1 1 1)	
0%	0.737		0.641		0.755	
1%	0.730	0.95%	0.636	0.78%	0.739	2.12%
2%	0.719	2.44%	0.624	2.65%	0.717	5.03%
3%	0.706	4.21%	0.609	4.99%	0.692	8.34%

Γ_{exp} denotes the surface energy calculated for the experimental lattice constant a_{exp}.

of the surface energies change by about the same percentage for all the surface orientations when the lattice parameter is decreased. In the case of Cu the theoretical LDA lattice constant is around 2% smaller than the experimental one, so that this effect changes the surface energy by less than 2.5%. However due to error cancellation the anisotropy ratio changes by less than 1.1%. For Ag and in general for the other 4d metals, Rh and Pd, the LDA lattice constants are about 1% smaller than the experimental lattice constants, while for the 5d metals the LDA values agree with the experimental lattice constants. Therefore the anisotropy ratios are independent of whether we use the LDA or the experimental lattice parameter. The following discussion of the anisotropy ratios would not change if we would have used the LDA instead of the experimental lattice constants in our calculations.

2.3. Relativistic effects

To study the importance of the relativistic effects we performed both non-relativistic (NR) and SR calculations. In Fig. 1 we present the surface energies for the three noble metals Cu, Ag and Au obtained using the FP. In the upper panel we have plotted the SR values while in the bottom panel the difference between the SR and the NR values.

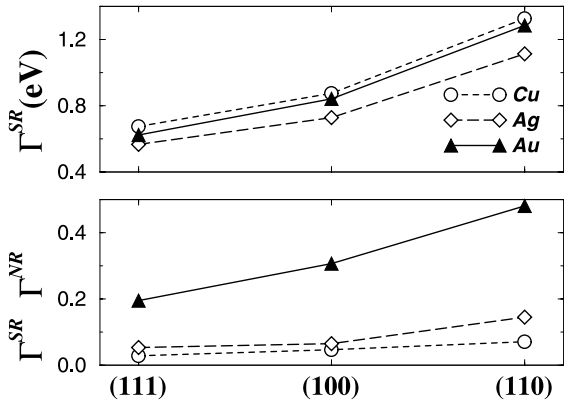

Fig. 1. Effect of relativity on the FP surface energies of the noble metals. In the upper panel we plot the SR surface energy, Γ^{SR}, in eV/atom and in the bottom panel the difference $\Gamma^{SR} - \Gamma^{NR}$, where NR stands for the NR calculations.

The main relativistic effect is to increase the surface energies and this effect is largest for Au being the heaviest element. In the NR calculations Au has the lowest surface energies of all three noble metals but in the SR calculations Au surface energies become comparable to the ones of Cu and the inclusion of spin–orbit coupling further increases them [29]. Also the anisotropy ratios are increased compared to NR values, by about 2–4% in the case of Cu and Ag and up to 8–10% in the case of Au.

3. Surface energies and anisotropy ratios

We have studied the surface energies of the low-index surfaces: (1 1 1), (1 0 0) and (1 1 0), and of the three most close-packed vicinal surfaces: (3 1 1), (3 3 1) and (2 1 0). From a slab calculation one can calculate the surface excess free energy at zero temperature from the relation

$$\Gamma = \frac{E_{\mathrm{slab}} - NE_{\mathrm{bulk}}}{2}, \tag{1}$$

where E_{slab} is the total energy of the slab, N is the total number of layers of the metal, E_{bulk} is the energy per atom in the bulk crystal. The factor 2 enters because a finite slab has two surfaces. To be consistent for all the cases we used as E_{bulk} the energy per atom of the central layer of the slab. The latter one differs from the energy of a bulk system by less than 10^{-4} eV, which results in changes in the surface energies of less than 1 meV.

The broken-bond-rule states [29] that the surface energy $\Gamma_{(hkl)}$ in eV/(surface atom) needed to create a surface with a Miller index (hkl) reduces just to the product of $\Gamma_{(111)}$ and the ratio of the first-neighbor broken bonds $N_{(hkl)}$ and $N_{(111)} = 3$:

$$\Gamma_{(hkl)} \cong \frac{N_{(hkl)}}{3}\Gamma_{(111)}. \tag{2}$$

$N_{(hkl)}$ can be easily obtained for any fcc surface [39]:

$$N_{(hkl)} = \begin{cases} 2h + k & h,k,l \text{ odd} \\ 4h + 2k & \text{otherwise} \end{cases} \quad h \geqslant k \geqslant l. \tag{3}$$

As a consequence the anisotropy ratios between the surface energy for an arbitrary surface orientation over the surface energy for the (1 1 1) surface orientation is close to the ratio between the number of broken bonds between nearest neighbors for these surfaces. Here we will study how well the paramagnetic fcc transition and sp metals satisfy the broken-bond rule for the surface energies. Here we should mention that in the case of the bcc materials a simple broken-bond rule is not expected as the distances of the next nearest and nearest neighbors are rather close. This is also obvious by looking to the pair-potentials data extracted from ab initio calculations in Ref. [28].

3.1. Transition metals

In Table 3 we have gathered our FP SR results for all the transition metal surfaces. The first comment on this table is pretty obvious. For all the metals the surface energy increases with the roughness of the surface, i.e. as the number $N_{(hkl)}$ of broken bonds increases, where (1 1 1) is the most close-packed surface with $N_{(111)} = 3$. Also the surface energies for an isoelectronic row increase for the heavier element; the surface energy of Pt is larger than the one of Pd. Presumably the explanation is that the Pt d-levels are higher in energy and d-wave functions are more extended than the Pd ones leading to stronger bonding. Also along a series in the periodic table the surface energy is at the end of the series larger for the compound with the smaller number of d-electrons. In the same table we present in parenthesis the anisotropy ratios. To open the (1 0 0) surface we break four nearest-neighbor bonds, for the (1 1 0) surface six bonds, for the (3 1 1) one seven bonds, the (3 3 1) one nine bonds and finally for the (2 1 0) one 10 bonds. So the ideal broken-bond ratios, R_{BB}, with

Table 3
FP SR surface energies for the six more closed-packed surfaces for the four transition metals

Γ (eV)	Pd	Pt	Rh	Ir	R_{BB}
(1 1 1)	0.822	0.957	1.034	1.200	
(1 0 0)	(1.28) 1.049	(1.33) 1.272	(1.36) 1.404	(1.42) 1.707	4/3
(1 1 0)	(1.94) 1.596	(2.06) 1.973	(1.98) 2.047	(2.07) 2.488	2
(1 1 3)	(2.28) 1.873	(2.40) 2.295	(2.35) 2.428	(2.43) 2.913	7/3
(3 3 1)	(2.93) 2.404	(2.98) 2.853	(2.99) 3.094	(3.04) 3.652	3
(2 1 0)	(3.22) 2.644	(3.30) 3.158	(3.35) 3.464	(3.48) 4.172	10/3

In parenthesis the anisotropy ratios with respect to the (1 1 1) surface, which are close to the ideal broken-bond ratios $R_{\mathrm{BB}} = \frac{N_{(hkl)}}{N_{(111)}}$ for these surfaces.

respect to the (1 1 1) surface, for which we break three nearest-neighbors bonds, are 4/3, 2, 7/3, 3 and 10/3, for the (1 0 0), (1 1 0), (3 1 1), (3 3 1) and (2 1 0) surface orientations respectively. The calculated surface energy anisotropy ratios deviate slightly from these ideal numbers. For Pd the calculated ratios are smaller than the ideal ones by ~3–4% for all the surface orientations, while the Ir ratios are larger from the ideals ones by ~4–7% for all the surface orientations except the (3 3 1) where the calculated Ir ratio is by 1.3% larger than the ideal ratio. Pt and Rh show a mixed behavior but in general the ratios differ less than 3% from the ideal nearest-neighbors broken-bonds ratios for any surface. So in general transition metal surfaces follow the broken-bond rule but with slightly larger deviations than the noble metals due to the fact that their d-band is not filled and they present peaks at the Fermi level, which can slightly change from one surface orientation to the other and consequently the energy needed to break a bond changes also slightly.

The results presented in the previous paragraph have been obtained taking into account the non-spherical part of the potential, i.e. known as the FP scheme. The use of the FP instead of the ASA accounts in a more accurate way for the charge distribution near the surface where due to the lower symmetry the charge exhibits larger variations than in the bulk. The use of FP lowers the energies compared to ASA by about 15% for all the surfaces under study. A similar behavior is also found for the vicinal surfaces. At first sight it seems that the ASA is efficiently accurate to describe the surface energies of the materials under study. However, the anisotropy ratios are more sensitive that the surface energies themselves. In Fig. 2 we have represented the anisotropy ratios for the noble and transition metals for the three low index and the three vicinal surfaces which we have studied. The straight lines represent the ideal broken-bonds ratios. We see that already for the Pd(3 1 1) surface the ASA produces a ratio that deviates strongly from the broken-bond rule while the FP is rather close. The differences become even more dramatic for the more open (3 3 1) and (2 1 0) surfaces. ASA produces for the Cu and Ir surfaces ratios that deviate strongly from the broken-bond

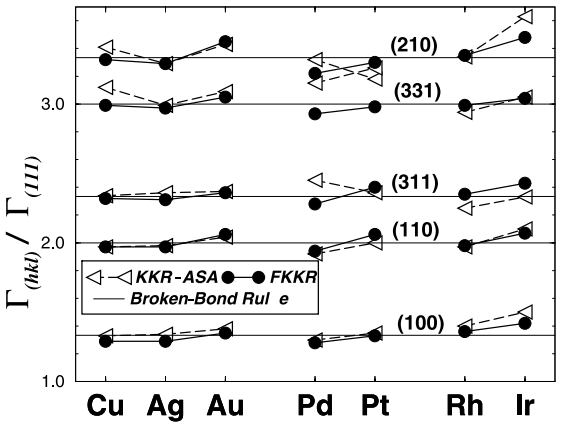

Fig. 2. Anisotropy ratios for the low index and the most close-packed vicinal surfaces within ASA and FP. For the vicinal surfaces the use of FP is necessary, due to the failure of ASA to describe accurately the more complex metal–vacuum interface.

rule while the FP restores the ideal ratios. Especially for Pd, the ASA predicts that the surface energy for the (3 3 1) surface is larger than the one for the (2 1 0) surface which is more open. The use of FP restores the broken-bond rule behavior. So although the ASA is sufficiently accurate to produce reasonable surface energies, the use of FP is decisive for the calculation of the anisotropy ratios of the vicinal surfaces.

In the previous discussion, the anisotropy ratio is always defined with respect to the energy of the (1 1 1) surface. Thus any errors in the (1 1 1) value is reflected directly in all ratios, in this way leading to an unwanted bias for all $(h\,k\,l)$ values. Moreover the (1 1 1) surface is the most close-packed surface exhibiting the smallest number of broken bonds. In Fig. 2 it seems that the (1 1 1) surface energy of Pd is slightly overestimated leading to anisotropy ratios systematically smaller than the ideal values, while in the case of Ir the (1 1 1) surface energy seems to be underestimated. Therefore is might be more reasonable to define an average broken-bond strength E_{BB} by dividing the calculated $\Gamma_{(h\,k\,l)}$ value by the number of broken bonds and average over all six orientations:

$$E_{\mathrm{BB}} = \frac{1}{6} \sum_{(h\,k\,l)} \frac{\Gamma_{(h\,k\,l)}}{N_{(h\,k\,l)}}. \tag{4}$$

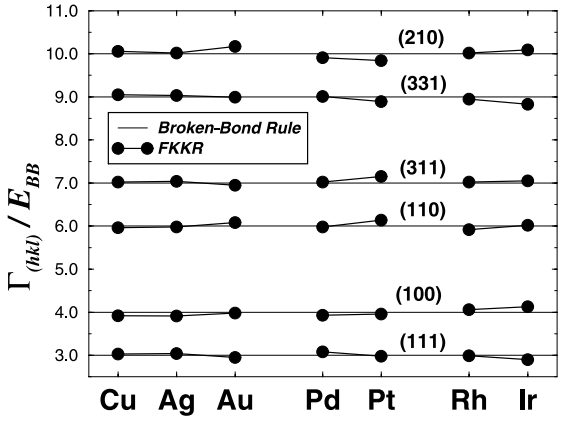

Fig. 3. Surface energy Γ in units of the average bond strength E_{BB} for the low-index and vicinal surfaces of the noble and transition metals.

This choice of E_{BB} is somewhat arbitrary but similar results are obtained if we take only the three low-index surfaces to define an average bond strength. Using the average bond strength defined in Eq. (4) we have plotted in Fig. 3 the ratio $\Gamma_{(hkl)}/E_{\mathrm{BB}}$, i.e. the surface energy $\Gamma_{(hkl)}$ in units of the average bond strength E_{BB}. This ratio can be interpreted as an effective number of broken bonds, which as Fig. 3 shows, agrees very well with the ideal number of broken bonds. The regularity of the data and the close agreement with the number of nearest-neighbors broken bonds $N_{(hkl)}$ shows a surprising simplicity in the surface energy of the fcc metals, which has not been detected previously.

The physical reason of the broken-bond rule can be elucidated by a TB model using similar arguments as used by Friedel for the cohesion energies. Following the presentation in Ref. [40], in a nearest-neighbor TB model the surface energy for a transition metal surface is given by

$$\Gamma \simeq \frac{W_{\mathrm{S}} - W_{\mathrm{B}}}{20} n_{\mathrm{d}}(n_{\mathrm{d}} - 10), \tag{5}$$

where n_{d} is the number of d-electrons and W_{S} and W_{B} are the band widths for the surface and bulk density of states, which have been approximated by rectangular forms. Since the band width scales with the coordination number, the surface energy is related to the cohesive energy E_{coh}

$$\Gamma \simeq \left(1 - \sqrt{\frac{Z_{\mathrm{S}}}{Z_{\mathrm{B}}}}\right) E_{\mathrm{coh}}, \tag{6}$$

where Z_{S} is the surface coordination number and Z_{B} the bulk one. Using $Z_{\mathrm{S}} = Z_{\mathrm{B}} - N_{(hkl)}$ and expanding the square root linearly in the number of broken bonds $N_{(hkl)}$, one obtains for the surface energy

$$\Gamma_{(hkl)} \simeq \frac{1}{2} \frac{N_{(hkl)}}{Z_{\mathrm{B}}} E_{\mathrm{coh}}. \tag{7}$$

As demonstrated in Ref. [40] the arguments can be refined by including an additional pair-potential term to describe the sp repulsion.

In Fig. 4 we have plotted the surface energy anisotropy ratios with respect to the (1 1 1) surface for the low-index surface together with the results by Vitos et al. from Ref. [25]. In contrast to the noble metals the values of Vitos et al. for the transition metals deviate only slightly from our results. In Ref. [29] we have explained the discrepancy for the noble metals as due to an insufficient number of $\mathbf{k}_{\parallel}$-points used in Ref. [25] in the evaluation of the BZ integrals. The (1 1 1) surface of the noble metals presents a surface state centered at the $\bar{\Gamma}$ point which can only be accounted for by a sufficiently dense grid. Such states do not occur for the fcc transition metals and thus the number of $\mathbf{k}_{\parallel}$-points used in Ref. [25] is sufficient

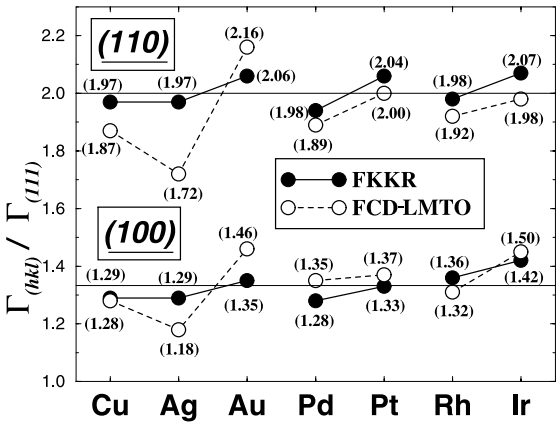

Fig. 4. Anisotropy ratios within both FKKR and LMTO from Ref. [25]. Contrary to the noble metals, whose (1 1 1) surfaces possess a surface state centered at the $\bar{\Gamma}$ point, the transition metals results are similar for both methods.

to produce accurate ratios, that agree well with our FP results. Since the authors of the Ref. [25] did not perform calculations for the vicinal surfaces, we cannot judge the behavior of the FCD-LMTO-ASA method for these more difficult cases.

As mentioned in the introduction there are several other ab initio calculations for the surface energies of these materials but they concern just one or two surfaces and thus allow no conclusions for the anisotropy ratios. In Table 4 we have

Table 4
Surface energies is $J\,m^{-2}$ for the three low-index surfaces of the paramagnetic fcc transition metals using the FKKR

γ ($J\,m^{-2}$)	FKKR	Ref. [25]	Other calculations	Experiments
Cu(1 1 1)	1.91	1.95	1.59[a], 1.94[b]	1.79[c], 1.83[d]
Cu(1 0 0)	2.15	2.17	1.71[a], 1.80[e]	
Cu(1 1 0)	2.31	2.24	1.85[a]	
Rh(1 1 1)	2.65	2.47	2.53[f], 2.85[g]	2.66[c], 2.70[d]
Rh(1 0 0)	3.12	2.80	2.81[f], 3.28[g], 2.65[h], 2.59[i]	
Rh(1 1 0)	3.22	2.90	2.88[f], 3.37[g]	
Pd(1 1 1)	2.01	1.92	1.64[f]	2.00[c], 2.05[d]
Pd(1 0 0)	2.22	2.33	1.86[f], 2.30[j], 2.13[k]	
Pd(1 1 0)	2.39	2.23	1.97[f], 2.50[j]	
Ag(1 1 1)	1.25	1.17	1.21[f]	1.25[c], 1.25[d]
Ag(1 0 0)	1.40	1.20	1.21[f], 1.30[j], 1.27[l], 1.11[m]	
Ag(1 1 0)	1.51	1.24	1.26[f], 1.40[j]	
Ir(1 1 1)	3.02	2.97	3.27[n]	3.05[c], 3.00[d]
Ir(1 0 0)	3.71	3.72		
Ir(1 1 0)	3.82	3.61		
Pt(1 1 1)	2.31	2.30	2.20[n], 2.07[o]	2.49[c], 2.48[d]
Pt(1 0 0)	2.65	2.73		
Pt(1 1 0)	2.91	2.82		
Au(1 1 1)	1.39	1.28	1.25[n], 1.04[p]	1.51[c], 1.50[d]
Au(1 0 0)	1.62	1.63	1.33[m], 1.30[q]	
Au(1 1 0)	1.75	1.70	1.43[r]	

In second column the results using the FCD-LMTO-ASA and on the third and fourth columns existing ab initio calculations and experiments.

[a] Pseudopotentials, Ref. [48].
[b] FP-LMTO, Ref. [49].
[c] Experiment, Ref. [2].
[d] Experiment, Ref. [3].
[e] Modified APW, Ref. [50].
[f] FP-LMTO, Ref. [10].
[g] Pseudopotentials, Ref. [51].
[h] Pseudopotentials, Ref. [52].
[i] FLAPW, Ref. [41].
[j] FLAPW, Ref. [53].
[k] Pseudopotentials, Ref. [54].
[l] FLAPW, Ref. [55].
[m] Pseudopotentials, Ref. [56].
[n] Pseudopotentials, Ref. [57].
[o] Pseudopotentials, Ref. [21].
[p] Pseudopotentials, Ref. [58].
[q] FLAPW, Ref. [59].
[r] Pseudopotentials, Ref. [60].

gathered the results from previous ab initio calculations and experiments. We have expressed all the results in $J\,m^{-2}$ and not in eV/atom, as experiment have been performed in the liquid phase of the metals. For the noble metals our and Vitos' results agree nicely when expressed in $J\,m^{-2}$, and the calculated values are very close to the experimental ones. The latter values are not orientation specific but averaged values and they should be closer to the most close-packed surface: the (1 1 1). Other calculations agree with our and Vitos databases. The FP-LMTO results by Methfessel and collaborators [10] agree nicely with ours except the case of Ag where they predict a jelliumlike behavior for the (1 1 1) and (1 0 0) surfaces, i.e. same surface energy per unit surface area, which is not expected for a noble metal. Finally our calculated surface energies are in reasonable agreement with previous TB calculations by Barreteau et al. [13] on the low-index surfaces of Rh and Pd and by Mehl and Papaconstantopoulos [14] on the ensemble of noble and transition metals.

We should mention that in our calculations we did not relax the positions of the layers but to a large extent this effect should not affect the surface energies [29]. We have shown in Ref. [29] that for the noble metals the (1 1 1) and (1 0 0) surface energies change less than 1%, when relaxations are taken into account. The (1 0 0)/(1 1 1) anisotropy ratio remained unchanged for Cu and decreased by about 1% and 1.5% for Ag and Au, respectively, compared to the unrelaxed values. Relaxations decreased the (1 1 0) surface energy of Cu and Ag by ~3% and ~2%, respectively, and the anisotropy ratios with respect to the (1 1 1) surface changed by about 1%. Even in the case of the (1 1 0) surface of Au that showed the largest relaxation and the surface energy decreased by more than ~6%, the calculated anisotropy ratio was 1.89 close to the ideal broken-bond rule value of 2. These results confirm the calculations of Feibelman and collaborators [41,42] and Mansfield and collaborators [43], who predicted by first-principle calculations that the effect of the relaxation on the calculated surface energy of a particular facet should be around 2–5% depending on the roughness of the facet. Surface relaxations for vicinal surfaces have been studied mainly using semi-empirical methods due to the complexity arisen by the simultaneous relaxation of a large number of layers [44]. Rodriguez and collaborators using such a semi-empirical method showed that surface relaxations affect typically the anisotropic ratios by less than 2% [16].

3.2. sp Metals

To complete our study we also investigated the sp metals Ca, Sr, Al and Pb that crystallize also in the fcc structure. In Table 5 we have gathered the FP surface energies and in parenthesis the anisotropy ratios for the six more close-packed surfaces. In general the surface energies for these materials are smaller than for the d-metals due to the fact that the bonds are made of s- and p-electrons that are more mobile than the localized d-electrons and so one needs less energy to break these bonds. This becomes even more clear when we look at the surface energy expressed in surface units (see Table 6). The Ca(1 0 0) and Sr(1 0 0) surfaces show a rather small anisotropy ratio compared to the transition and noble metals and also compared to Al.

Table 5
FP SR surface energies for the six more closed-packed surfaces of the four sp metal

Γ (eV)	Ca	Sr	Al	Pb	R_{BB}
(1 1 1)	0.417	0.373	0.489	0.398	
(1 0 0)	(1.21) 0.503	(1.22) 0.454	(1.28) 0.625	(1.24) 0.492	4/3
(1 1 0)	(1.92) 0.797	(1.94) 0.722	(1.93) 0.943	(1.95) 0.778	2
(3 1 1)	(2.27) 0.946	(2.27) 0.847	(2.24) 1.094	(2.18) 0.866	7/3
(3 3 1)	(2.96) 1.234	(2.93) 1.094	(2.94) 1.436	(2.81) 1.118	3
(2 1 0)	(3.20) 1.333	(3.18) 1.187	(3.20) 1.565	(3.53) 1.405	10/3

In parenthesis the anisotropy ratios with respect to the (1 1 1) surface, which are close to the ideal broken-bond ratios R_{BB} for these surfaces.

Table 6
Surface energies is $J\,m^{-2}$ for the three low-index surfaces of the paramagnetic fcc sp metals using the FKKR

γ ($J\,m^{-2}$)	FKKR	Ref. [25]	Other calculations	Experiments
Ca(1 1 1)	0.50	0.57		0.50[a], 0.49[b]
Ca(1 0 0)	0.52	0.54		
Ca(1 1 0)	0.58	0.58		
Sr(1 1 1)	0.37	0.43		0.42[a], 0.41[b]
Sr(1 0 0)	0.39	0.41		
Sr(1 1 0)	0.44	0.43		
Al(1 1 1)	1.10	1.12	0.94[c], 1.12[d]	1.14[a], 1.12[b]
Al(1 0 0)	1.22	1.35	1.08[c], 1.14[d]	
Al(1 1 0)	1.30	1.27	1.09[c], 1.28[d]	
Pb(1 1 1)	0.60	0.32	0.50[e]	0.59[a], 0.60[b]
Pb(1 0 0)	0.64	0.38		
Pb(1 1 0)	0.72	0.45	0.59[e]	

In second column the results using the FCD-LMTO-ASA and on the third and fourth columns existing ab initio calculations and experiments.
[a] Experiment, Ref. [2].
[b] Experiment, Ref. [3].
[c] Pseudopotentials, Ref. [46].
[d] Pseudopotentials, Ref. [47].
[e] Pseudopotentials, Ref. [43].

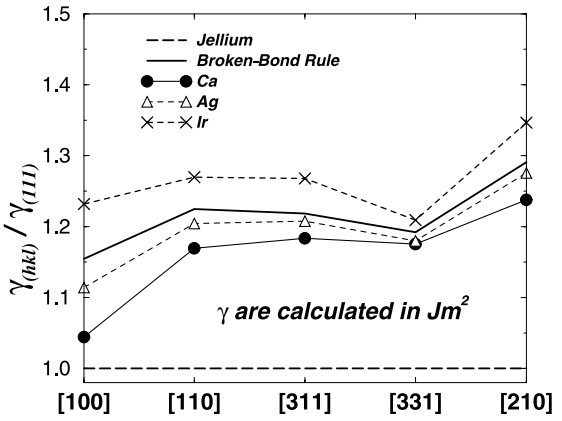

Fig. 5. Anisotropy ratios but calculating the surface energies in $J\,m^{-2}$ for Ag, Ir and Ca. The solid line corresponds to the broken-bond rule and the tilted one to the jellium. The Ca(1 0 0) surface is close to jellium but then it recovers the Ag and Ir behavior.

Ca and Sr are in the periodic table just near the simple metals which are known to be well described by a simple jellium model [45]. So we expect that to some extent we should find a jelliumlike behavior also for the Ca and Sr surfaces, at least for the low-index ones. This is really what happens. In Fig. 5 we represent the anisotropy ratios but now taking into account the energy per surface area ($J\,m^{-2}$) and not per atom (eV/atom). For a jellium model the surface energy per surface area would be constant for any surface and the anisotropy ratio would be always 1. With the solid line we represent the anisotropy ratios if the broken-bond rule is applicable, and the ratios for Ca, Ag and Ir. Ag is closer to the broken-bond rule than Ir where the ratios are always overestimated. For the Ca(1 0 0) surface we see that the value is closer to the jellium model but for the more open surfaces the anisotropy ratios are closer to the broken-bond model than the jellium.

Contrary to Ca and Sr, Al shows the same behavior as Pd and the calculated ratios are slightly smaller than the ideal ones (see Table 5). The most interesting case is Pb. For the (1 0 0) and (1 1 0) surfaces the ratios are near to the Sr ones while for the next two vicinal surface orientations, (3 1 1) and (3 3 1), the calculated anisotropy ratios are more than 6% smaller than the ideal values. But for the (2 1 0) surface the anisotropy ratio changes the behavior and now is larger by 6% than the ideal value of 10/3. This is an indication that the behavior of Pb is more complicated than all the other fcc metals we have studied in this contribution. Here we have to mention that the surface energies in Table 5 have been calculated taking the 5d as valence electrons as they are located just below the sp bands. We recalculated the surface energies of Pb considering the 5d as core states, by increasing the number of layers, the number of energy points used to do the integrations in the complex energy plane and finally the number of $\mathbf{k}_{\parallel}$-points. Although the surface energies changed slightly due to the core treatment of the 5d states, the anisotropy ratios were extremely stable. One plausible explanation for the different behavior of Pb compared to the other sp materials is the possibility that for such a heavy element the SR approximation is not appropriate since it does not include the spin–orbit coupling.

In Table 6 we have gathered our calculated surface energies in $J\,m^{-2}$ together with other calculations and experiments. Our results agree nicely

with the Vitos et al. database in Ref. [25] with the exception of Pb where our surface energy per surface area is double as high, but our results agree nicely with previous calculations by Mansfield and Needs [43] using pseudopotentials and the existing experimental data. Both Schöchlin et al. [46] and Stumpf and Scheffler [47] have studied all the three low-index surfaces of Al. Comparing Schöchlin et al. calculations with Stumpf's and Scheffler's results we see that the former calculations predict comparable surface energies for the (1 0 0) and (1 1 0) surfaces while the latter ones predict comparable surface energies for the (1 1 1) and (1 0 0) surfaces. Both calculations are in contradiction to our calculations which predict a considerable increase of the surface energy as the surface becomes more open, while the calculations in Ref. [25] state that the surface energy per surface area is smaller for the (1 1 0) surface compared to the (1 0 0) surface. This spread of the results for Al does not allow us to draw safe conclusions for the variation of the surface energy with the surface orientation.

4. Conclusions

We have shown using the FP screened KKR code that the broken-bond rule, i.e. the linear scaling of the surface energy with the number of nearest-neighbors broken bonds, is not only valid for the noble metals [29] but also for the fcc transition metals. For the sp metals the (1 1 1) and (1 0 0) surfaces show a jelliumlike behavior but for the more open surfaces the surface energies follow again the broken-bond rule with Pb presenting the largest deviations. The use of the FP instead of the full-charge ASA decreases the surface energies and is essential for an accurate calculation of the anisotropy ratios for the vicinal surfaces. In total the surface energies of the fcc metals show an astonishingly simple anisotropy behavior which has not been recognized previously.

Acknowledgements

Authors gratefully acknowledge support from the RT Network of Computational Magnetoelectronics (contract no: RTN1-1999-00145) of the European Commission.

References

[1] V.K. Kumikov, Kh.B. Khokonov, J. Appl. Phys. 54 (1983) 1346.
[2] W.R. Tyson, W.A. Miller, Surf. Sci. 62 (1977) 267.
[3] F.R. Boer, R. Boom, W.C.M. Mattens, A.R. Miedema, A.K. Niessen, Cohesion in Metals, North-Holland, Amsterdam, 1988.
[4] B.E. Sundquist, Acta Met. 12 (1964) 67;
W.L. Winterbottom, N.A. Gjostein, Act. Met. 14 (1966) 1041;
J.C. Heyraud, J.J. Métois, Acta Met. 28 (1980) 1789;
Z. Wang, P. Wynblatt, Surf. Sci. 398 (1998) 259.
[5] U. Breuer, H.P. Bonzel, Surf. Sci. 273 (1992) 219.
[6] J.C. Heyraud, J.J. Metois, Surf. Sci. 128 (1983) 334;
J.C. Heyraud, J.J. Metois, Surf. Sci. 177 (1986) 213.
[7] G. Bilalbegivić, F. Ercolessi, E. Tosatti, Surf. Sci. 280 (1993) 335;
H.M. van Pixteren, J.W.M. Frenken, Europhys. Lett. 21 (1993) 43;
H.M. van Pixteren, B. Pluis, J.W.M. Frenken, Phys. Rev. B 49 (1994) 13798.
[8] H.P. Bonzel, K. Dückers, Surf. Sci. 184 (1987) 425.
[9] H.P. Bonzel, A. Edmundts, Phys. Rev. Lett. 84 (2000) 5804.
[10] M. Methfessel, D. Hennig, M. Scheffler, Phys. Rev. B 46 (1992) 4816.
[11] H.L. Skriver, N.M. Rosengaard, Phys. Rev. B 46 (1992) 7157.
[12] J. Kollár, L. Vitos, H.L. Skriver, Phys. Rev. B 49 (1994) 11288.
[13] C. Barreteau, D. Spanjaard, M.C. Desjonquères, Surf. Sci. 433–435 (1999) 751.
[14] M.M. Mehl, D. Papaconstantopoulos, Phys. Rev. B 54 (1996) 4519.
[15] S.M. Foiles, M.I. Baskes, M.S. Daw, Phys. Rev. B 33 (1996) 7983;
G.J. Ackland, G. Tichy, V. Vitek, M.W. Finnis, Philos. Mag. A 56 (1987) 735;
D. Wolf, Surf. Sci. 226 (1990) 389;
M.I. Baskes, Phys. Rev. B 46 (1992) 2727;
P. van Beurden, G.J. Kramer, Phys. Rev. B 63 (2001) 165106.
[16] A.M. Rodríguez, G. Bozzolo, J. Ferrante, Surf. Sci. 289 (1993) 100.
[17] P. Hohenberg, W. Kohn, Phys. Rev. 136 (1964) B864;
W. Kohn, L.J. Sham, Phys. Rev. 140 (1965) A1133.
[18] U. von Barth, L. Hedin, J. Phys. C 5 (1972) 1629.
[19] H.L. Skriver, N.M. Rosengaard, Phys. Rev. B 43 (1991) 9538.
[20] M. Alden, H.L. Skriver, S. Mirbt, B. Johansson, Phys. Rev. Lett. 69 (1992) 2296;

M. Alden, H.L. Skriver, S. Mirbt, B. Johansson, Surf. Sci. 315 (1994) 157.
[21] P.J. Feibelman, Phys. Rev. B 52 (1995) 16845.
[22] L. Vitos, J. Kollár, H.L. Skriver, Phys. Rev. B 55 (1997) 13521.
[23] O.K. Andersen, O. Jepsen, Phys. Rev. Lett. 53 (1984) 2671; O.K. Andersen, O. Jepsen, M. Sob, in: M. Yussouf (Ed.), Electronic Band Structure its Applications, Springer, Berlin, 1987.
[24] J.P. Perdew, K. Burke, M. Ernzerhof, Phys. Rev. Lett. 77 (1996) 3865.
[25] L. Vitos, A.V. Ruban, H.L. Skriver, J. Kollár, Surf. Sci. 411 (1998) 186.
[26] L. Vitos, J. Kollár, H.L. Skriver, Phys. Rev. B 49 (1994) 16694.
[27] J.A. Moriarty, R. Phillips, Phys. Rev. Lett. 66 (1991) 3036.
[28] L. Vitos, H.L. Skriver, J. Kollár, Surf. Sci. 425 (1999) 212.
[29] I. Galanakis, G. Bihlmayer, V. Bellini, N. Papanikolaou, R. Zeller, S. Blügel, P.H. Dederichs, Europhys. Lett., in press. Available from <arXiv:cond-mat/0105207>
[30] V. Bellini, N. Papanikolaou, R. Zeller, P.H. Dederichs, Phys. Rev. B 64 (2001) 094403.
[31] S.H. Vosko, L. Wilk, N. Nusair, Can. J. Phys. 58 (1980) 1200.
[32] R. Zeller, P.H. Dederichs, B. Újfalussy, L. Szunyogh, P. Weinberger, Phys. Rev. B 52 (1995) 8807; N. Papanikolaou, R. Zeller, P.H. Dederichs, J. Phys.: Condens. Matter 14 (2002) 2799.
[33] O.K. Andersen, Z. Pawlowska, O. Jepsen, Phys. Rev. B 34 (1986) 5253.
[34] N. Stefanou, H. Akai, R. Zeller, Comp. Phys. Commun. 60 (1990) 231.
[35] R. Zeller, Phys. Rev. B 55 (1997) 9400; K. Wildberger, R. Zeller, P.H. Dederichs, Phys. Rev. B 55 (1997) 10074.
[36] R. Zeller, J. Deutz, P.H. Dederichs, Solid State Commun. 44 (1982) 993; K. Wildberger, P. Lang, R. Zeller, P.H. Dederichs, Phys. Rev. B 52 (1995) 11502.
[37] H.J. Monkhorst, J.D. Pack, Phys. Rev. B 13 (1976) 5188.
[38] N.W. Ashcroft, N.D. Mermin, Solid State Physics, Saunders College Publishing, 1976.
[39] J.K. Mackenzie, A.J.W. Moore, J.F. Nicholas, J. Phys. Chem. Solids 23 (1962) 185.
[40] M.C. Desjonquères, D. Spanjaard, in: Concepts in Surface Physics, Springer Series in Surface Science, vol. 30, Springer-Verlag, Berlin, Heidelberg, 1993.
[41] P.J. Feibelman, D.R. Hamann, Surf. Sci. 234 (1990) 377.
[42] P.J. Feibelman, Phys. Rev. B 46 (1992) 2532.
[43] M. Mansfield, R.J. Needs, Phys. Rev. B 43 (1991) 8829.
[44] J. Wan, Y.L. Fan, D.W. Gong, S.G. Shen, X.Q. Fan, Modell. Simul. Mater. Sci. Eng. 7 (1999) 189, and references therein.
[45] N.D. Lang, W. Kohn, Phys. Rev. B 1 (1970) 4555; J.P. Perdew, R. Monniert, Phys. Rev. Lett. 37 (1976) 1286; R. Monniert, J.P. Perdew, Phys. Rev. B 17 (1978) 2595; Z.Y. Zhang, D.C. Langreth, J.P. Perdew, Phys. Rev. B 41 (1990) 5674; J.P. Perdew, H.Q. Tran, E. Smith, Phys. Rev. B 42 (1990) 11627; K.F. Wojciechowski, Surf. Sci. 437 (1999) 285.
[46] J. Schöchlin, K. Bohnen, K.M. Ho, Surf. Sci. 324 (1995) 113.
[47] R. Stumpf, M. Scheffler, Phys. Rev. B 53 (1996) 4958.
[48] Th. Rodach, K.P. Bohnen, K.M. Ho, Surf. Sci. 286 (1993) 66.
[49] H.M. Polatoglou, M. Methfessel, M. Scheffler, Phys. Rev. B 48 (1993) 1877.
[50] H. Bross, M. Kauzmann, Phys. Rev. B 51 (1995) 17135.
[51] A. Eichler, J. Hafner, J. Furthmüller, G. Kresse, Surf. Sci. 346 (1996) 300.
[52] L. Morrison, D.M. Bylander, L. Kleinman, Phys. Rev. Lett. 71 (1993) 1083.
[53] M. Weinert, R.E. Watson, J.W. Davenport, G.W. Fernando, Phys. Rev. B 39 (1989) 12585.
[54] A. Wachter, K.P. Bohnen, K.M. Ho, Surf. Sci. 346 (1996) 127.
[55] H. Erschbaumer, A.J. Freeman, C.L. Fu, R. Podloucky, Surf. Sci. 243 (1991) 317.
[56] N. Takeuchi, C.T. Chan, K.M. Ho, Phys. Rev. B 43 (1991) 14363.
[57] R.J. Needs, M. Mansfield, J. Phys.: Condens. Matter 1 (1989) 7555.
[58] N. Takeuchi, C.T. Chan, K.M. Ho, Phys. Rev. B 43 (1991) 13899.
[59] R. Eibler, H. Erschbaumer, C. Temnitschka, R. Podloucky, A.J. Freeman, Surf. Sci. 280 (1993) 398.
[60] K.M. Ho, K.P. Bohnen, Phys. Rev. Lett. 59 (1987) 1833.